Journal of Applied Geophysics 112 (2015) 206–214

Contents lists available at ScienceDirect

Journal of Applied Geophysics

journal homepage: www.elsevier.com/locate/jappgeo

Quality-factor and reflection-coefficient estimation using surface-wave ghost reflections from subvertical structures

Deyan Draganov [a,*], Elmer Ruigrok [b,1,2], Ranajit Ghose [a], Dylan Mikesell [c], Kasper van Wijk [d]

[a] Department of Geoscience & Engineering, Delft University of Technology, Stevinweg 1, 2628 CN Delft, The Netherlands
[b] Department of Earth Sciences, Utrecht University, Budapestlaan 4, 3584 CD Utrecht, The Netherlands
[c] Department of Earth, Atmospheric and Planetary Sciences, Massachusetts Institute of Technology, 77 MA Avenue, Cambridge, USA
[d] Department of Physics, The University of Auckland, 38 Princes Street, Auckland, New Zealand

ARTICLE INFO

Article history:
Received 29 August 2014
Accepted 25 November 2014
Available online 2 December 2014

Keywords:
Seismic interferometry
Surface waves
Intrinsic attenuation
Quality factor
Reflection coefficient
Ultrasonic

ABSTRACT

Seismic interferometry can retrieve the Green's function between receivers from the cross-correlation and summation of recordings from a boundary of surrounding sources. Having the sources only along a boundary is sufficient if the medium is lossless. If the medium is dissipative, the retrieved result using cross-correlation contains non-physical (ghost) arrivals. When using receivers at the surface and transient sources in the subsurface for the retrieval of the reflection response in a dissipative medium, it has been shown that the retrieved ghost reflections are characteristic of the quality factor of the subsurface. The ghost reflections are caused by internal reflections inside subsurface layers. It has been shown with numerical examples for recordings in a borehole from a surface source that a ghost reflection can be discriminated from physical reflections and tied to a specific subsurface layer. After connecting the ghost reflection to a specific layer, the quality factor of the medium above this layer and the reflection coefficient at the layer interface can be estimated. In this article, we show how the above principles can be adapted and applied for surface waves. Due to intrinsic losses in the medium, surface-wave ghost reflections are retrieved from internal scattering between subvertical boundaries. We demonstrate the method on an ultrasonic dataset recorded on a sample composed of a PVC block and an aluminum block. The aluminum block has a groove parallel to the PVC/aluminum interface. Using a surface-wave ghost reflection between the groove and the PVC/aluminum interface, we estimate the quality factor of the PVC and the reflection coefficient at the PVC/aluminum interface. We also show that the ghost reflection can be identified and tied to the layer between the groove and the PVC/aluminum interface, thus confirming previous numerical findings.

1. Introduction

When propagating through the earth, the seismic waves experience intrinsic losses due to internal friction, viscous drag and other mesoscopic and microscopic mechanisms. The effect of the loss of energy can be expressed by the dimensionless quantity Q, which is called quality factor. Determining spatially detailed knowledge of Q is important for accurate interpretation of processes inside the earth and the composition of the earth at different scales. For example, Solomon (1972) showed that the knowledge of the Q-values for Rayleigh and Love waves can be used to interpret partial melting in the upper mantle; Klimentos (1995) showed that the ratio of the Q-values for P- and S-waves can be used to distinguish between gas and condensate from oil and water saturation in reservoir rocks; Zhubayev and Ghose (2012a,b), showed that a joint inversion of frequency-dependent P- and S-wave velocity and their Q-values could be used for characterization of the flow properties in water-saturated soils.

A traditional method for estimating Q is the spectral-ratio method (e.g. Jannsen et al., 1985; Portsmouth et al., 1993; Tonn, 1991). It can be applied to transmission measurements using recordings at multiple seismic receivers from the same seismic source (common-shot gather) or from multiple sources at the same receiver (common-receiver gather). In both of these cases, the ratio between the spectra of the direct arrivals is computed and then used to estimate the Q-value of the medium between the receivers or between the sources. The method can also be applied to a measurement at a single receiver from a single source. In this case, the spectral ratio is estimated between a direct arrival and a primary reflection, which has reflected at a boundary. When only one reflector is present, the Q-value is estimated between the receiver and the reflector. The same technique could be used on a multilayer sample (subsurface), but in this case, the Q-estimate would be the

* Corresponding author at: Department of Geoscience & Engineering, Delft University of Technology, Stevinweg 1, 2628 CN Delft, The Netherlands. Tel.: +31 152786011.
E-mail addresses: d.s.draganov@tudelft.nl (D. Draganov), e.n.ruigrok@uu.nl (E. Ruigrok), r.ghose@tudelft.nl (R. Ghose), mikesell@mit.edu (D. Mikesell), k.vanwijk@auckland.ac.nz (K. van Wijk).
[1] Currently.
[2] Previously: Department of Geoscience & Engineering, Delft University of Technology, Stevinweg 1, 2628 CN, Delft, The Netherlands.

http://dx.doi.org/10.1016/j.jappgeo.2014.11.019
0926-9851/

apparent quality factor of the medium between the receiver and the reflector whose reflection is used.

Recently, Draganov et al. (2010) proposed an alternative method for estimating Q. This method makes use of non-physical arrivals retrieved from seismic interferometry with transient sources. Seismic interferometry is a method that allows the retrieval of the Green's function between two receivers, as if one of them were a source, using recordings from sources that effectively surround the receivers (e.g. Campillo and Paul, 2003; Schuster, 2001; Schuster et al., 2004; Snieder, 2004; Wapenaar, 2004; Wapenaar et al., 2002). The retrieval is most popularly performed by the process of cross-correlation: recordings at the two receivers from all surrounding sources are cross-correlated and the resulting correlations are summed over all sources to obtain the final retrieved Green's function. The theory with cross-correlation, with sources on a surrounding boundary, is derived for lossless media. When a medium causes intrinsic losses, the retrieved result will also contain non-physical (ghost) arrivals. When seismic interferometry is applied to receivers at the surface to retrieve the reflection response of the subsurface using subsurface boundary sources, the ghost events would be in the form of reflections that appear to have propagated only inside a subsurface layer and measured with source and receiver directly on top of that layer. In the correlation process, the ghost reflections are retrieved from arrivals that have experienced single or multiple reflections inside that layer. Draganov et al. (2010), used such body-wave ghost reflections to estimate Q of the medium above each subsurface layer, from inside which a ghost reflection is retrieved. The accuracy of their estimated values would depend on the signal-to-noise ratio of the later arrivals in the recordings that have experienced multiple reflections inside the layers in question. As a remedy, Ruigrok (2012) proposed to utilize only the earliest such arrivals, and using their amplitudes, the author estimated Q above and the reflection coefficient at the top of a layer that caused a ghost to be retrieved. When the subsurface is homogeneous or contains only one layer above a homogeneous half space, ghost reflections would not be retrieved even when there are intrinsic losses in the medium.

The loss-related ghost reflections are akin to the spurious reflections that appear in lossless media due to one-sided illumination of the receivers from an open boundary of sources (Draganov et al., 2012; King and Curtis, 2012; King et al., 2011; Snieder et al., 2006). Note that in media with intrinsic losses, ghost reflections would appear in the retrieved Green's function even when the transient sources effectively surround the receivers.

In the following, we show how the method from Ruigrok (2012) can be adapted and applied to estimate the surface-wave Q-value of the subsurface. This method can be seen as an alternative to the spectral-ratio method for cases when the latter method alone does not provide sufficiently reliable results. This might be the case when the recording geometry consists of sparse receivers in a medium with lateral changes in the seismic parameters, e.g. in volcanic settings or in the presence of a subvertical fault zone (e.g. Ghose et al., 2013). In such cases, the spectral-ratio method should be applied at single stations to estimate the Q-value between the station and a reflector, thus using a direct and a reflected arrival, to avoid erroneous results when the different receivers would be in media characterized by different intrinsic losses. In such cases, the method we propose could be applied at the same stations to obtain an alternative estimate of the Q-value. As will be shown in the last section, with our method we also estimate the reflection coefficient of the reflecting boundary, which supplies extra information about the media.

2. Method

For the explanation of the method we propose, we use the sketch in Fig. 1. It represents a plan view of a recording geometry with a seismic receiver (triangle) and two transient sources of plane waves (gray and black starts) placed at the earth's surface. The model consists of three

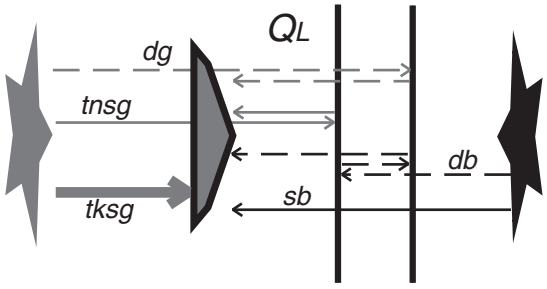

Fig. 1. Plan view of a vertically homogeneous earth model with a receiver (triangle) and two plane-wave sources (gray and black stars) at the surface, where the two thick black lines depict two reflective interfaces. The sources and receiver are elongated to illustrate the different arrivals. The symbol Q_L indicates that there are intrinsic losses in the left layer. The abbreviations label arrivals following different travel paths (arrows): sb — solid black; db — dashed black; tksg — thick solid gray; tnsg — thin solid gray; dg — dashed gray.

vertical layers separated by two vertical interfaces (thick black lines). This makes the model 1D for surface wave. Because the model is vertically homogeneous, propagating surface waves will not experience dispersion.

By applying seismic interferometry using cross-correlation to the recordings at the receiver from the two sources, we obtain a retrieved recording at the receiver from a virtual source collocated with it. To retrieve the surface-wave part of the Green's function, we would need to effectively surround the receiver, i.e. we need to have recordings from transient sources on each side of the receiver. If surface waves experience dispersion, to retrieve all the modes of the surface waves using cross-correlation correctly, the theory requires that also recordings be made from sources in the shallow subsurface down to a depth, at which the eigenfunctions become negligible. When only sources at the surface are used, only the fundamental mode of the surface wave will be retrieved correctly (Kimman and Trampert, 2010). For retrieval of the fundamental mode of the surface wave by seismic interferometry using cross-correlation from the surrounding transient sources, the arrivals at the receiver from each of the two sources need to be recorded separately. Then, the recordings from each source are correlated (in our case autocorrelated) separately and the two correlation results are summed.

To correctly retrieve the fundamental mode of the surface wave, the two plane-wave sources should have the same strength, same source mechanism (i.e. radiation pattern) and should emit energy with the same frequency content. As we assume plane-wave sources, there is no geometrical spreading, and the damping of the energy depends on transmission and reflection at parameter discontinuities and on the presence of intrinsic losses. Correlation of the direct (thick solid gray) arrival with the reflected (thin solid gray) arrival from the left interface of the middle layer will effectively eliminate the common travel path of the two arrivals (the thick solid gray path) and will retrieve a physical reflected surface wave. Note that the source in the right layer does not contribute to the retrieval of the physical reflection. Correlation of the thin solid gray with the dashed gray (the reflection from the right interface of the middle layer) arrivals will eliminate their common travel path. This will result in a retrieval of a reflected surface wave that kinematically would appear to have propagated only inside the middle layer. As such an arrival cannot be physically measured with collocated source and receiver at the position of the physical receiver, we call the arrival a non-physical (ghost) reflection. Correlation of the solid black with the dashed black arrival will also result in the retrieval of a ghost reflection from inside the middle layer. This ghost reflection, though, will have an opposite polarity compared to the gray ghost reflection. In the summation process of the correlated results from the two sources, the two retrieved ghost reflections will interact destructively. Together

with the destructive interference of their correlated multiples, this will result in the total disappearance of the ghost reflection. Thus, the right source only contributes to the suppression of retrieved ghost arrivals.

When the medium is dissipative, as indicated by the symbol Q_L in the left layer (L standing for left), the ghost surface-wave reflection will still be present in the retrieved result. This will happen because the thin solid gray and the dashed gray arrivals experience more damping than the black arrivals due to the longer paths of the former in the lossy left layer. Consequently, the ghost reflection retrieved from the correlation of the black arrivals will be stronger than the one retrieved from the correlation of the gray arrivals. In the following, we use the gray and black arrivals, which contribute to the retrieval of the ghost reflection, to estimate the Q-value in the left layer and the reflection coefficient at the left interface.

If the model would contain more vertical layers to the right of the middle layer, to make use of the gray and black arrivals and tie the estimated Q-value to the left layer, the ghost reflections will need to be identified as caused by the middle layer. This is possible if the source responses are recorded at extra receivers along a line crossing the different layers. Using the extra receivers, we can adapt the ghost-identification method from Draganov et al. (2013) to the situation from Fig. 1. The response from the left (gray) source measured at the different receiver positions is autocorrelated. If the retrieved ghost reflection has one polarity at a receiver in the left layer, but an opposite polarity for the receivers in the other two layers, then the ghost is caused by the middle layer.

To estimate Q and the reflection coefficient, Ruigrok (2012) used the amplitudes of body-wave arrivals at a surface receiver due to the same subsurface source. An extra complication arises in our case in that we have two sources on opposite sides of a receiver. Waves from the source left of the receiver will experience stronger or weaker attenuation depending on the source's distance from the receiver. This will result in the estimation of an erroneous Q-value. To avoid this, we propose to apply a simple amplitude normalization to the recordings.

To understand the normalization, let us look at the amplitudes of the different arrivals involved in the retrieval of the ghost reflection. The amplitude of the thick solid gray (tksg) arrival at the receiver position can be written as

$$A_{tksg}=A_{ls}e^{-\frac{t_{tksg}2\pi f_0}{Q_L}}, \tag{1}$$

where A_{ls} is the amplitude of the left source, t_{tksg} is the travel time of the thick solid gray arrival from the left source to the receiver, f_0 is the dominant frequency of the wave, and the amplitude damping due to the intrinsic losses is $e^{-\frac{t_{tksg}2\pi f_0}{Q_L}}$ (e.g. Aki and Richards, 2002). Using the same notation, the amplitudes of the thin solid gray (tnsg) and the dashed gray (dg) arrivals are

$$A_{tnsg}=A_{tksg}e^{-\frac{t_1 2\pi f_0}{Q_L}}r_{LM}e^{-\frac{t_1 2\pi f_0}{Q_L}} \tag{2}$$

and

$$A_{dg}=A_{tksg}e^{-\frac{t_1 2\pi f_0}{Q_L}}T_{LM}e^{-\frac{t_2 2\pi f_0}{Q_M}}r_{MR}e^{-\frac{t_2 2\pi f_0}{Q_M}}T_{ML}e^{-\frac{t_1 2\pi f_0}{Q_L}}, \tag{3}$$

respectively. In Eqs. (2) and (3), t_1 is the one-way travel time from the receiver to the left interface of the middle layer, t_2 is the one-way travel time inside the middle layer, Q_M is the quality factor of the middle layer (if it also causes intrinsic losses), r_{LM} and r_{MR} are the plane-wave reflection coefficients at the left and right boundaries of the middle layer, respectively, for a wave propagating from left to right, and T_{LM} and T_{ML} are the plane-wave transmission coefficients from the left to the middle layer and from the middle to the left layer, respectively. Each of the arrivals depends on the distance between the left source and the receiver only through the term A_{tksg}. This means that by normalizing the trace recorded due to the left source by the amplitude A_{tksg}, the dependance on the source–receiver distance and on the source strength is eliminated. In this way, the normalized amplitudes from Eqs. (2) and (3) become

$$A_{tnsg}^{norm}=e^{-\frac{t_1 2\pi f_0}{Q_L}}r_{LM}e^{-\frac{t_1 2\pi f_0}{Q_L}} \tag{4}$$

and

$$A_{dg}^{norm}=e^{-\frac{t_1 2\pi f_0}{Q_L}}T_{LM}e^{-\frac{t_2 2\pi f_0}{Q_M}}r_{MR}e^{-\frac{t_2 2\pi f_0}{Q_M}}T_{ML}e^{-\frac{t_1 2\pi f_0}{Q_L}}. \tag{5}$$

Similarly, we also normalize the trace at the receiver due the right source. Normalization means that the amplitudes of the solid black (sb) and the dashed black (db) arrivals become

$$A_{sb}^{norm}=1 \tag{6}$$

and

$$A_{db}^{norm}=r_{ML}e^{-\frac{t_2 2\pi f_0}{Q_M}}r_{MR}e^{-\frac{t_2 2\pi f_0}{Q_M}}, \tag{7}$$

respectively.

Eq. (4) gives a relation between the amplitudes of arrivals that we can measure and Q_L and r_{LM}. To solve for these two quantities, another relation is needed. We obtain such a relation using the amplitudes of the arrivals that in the correlation process contribute to the retrieval of the ghost reflection. Correlation of two arrivals is equivalent to the multiplication of their amplitudes. Thus, the correlation of the normalized surface-wave reflections from the left and right interfaces of the middle layer due to the left source, which correspond to the thin solid gray and the dashed gray arrivals in Fig. 1, means multiplication of Eqs. (4) and (5):

$$A_{tnsg}^{norm}*A_{dg}^{norm}=e^{-4\frac{t_1 2\pi f_0}{Q_L}}r_{LM}e^{-2\frac{t_2 2\pi f_0}{Q_M}}T_{LM}r_{MR}T_{ML}. \tag{8}$$

Using the normalized Eqs. (6) and (7), the correlation of the solid black and the dashed black arrivals due to the right source, i.e., the correlation of the normalized direct surface wave and its multiple, which has bounced between the left and the right interfaces, would give

$$A_{sb}^{norm}*A_{db}^{norm}=r_{ML}e^{-2\frac{t_2 2\pi f_0}{Q_M}}r_{MR}. \tag{9}$$

Dividing Eq. (8) by Eq. (9) and using $r_{ML}=-r_{LM}$, we obtain

$$\frac{A_{tnsg}^{norm}*A_{dg}^{norm}}{A_{sb}^{norm}*A_{db}^{norm}}=-e^{-4\frac{t_1 2\pi f_0}{Q_L}}T_{LM}T_{ML}. \tag{10}$$

Using the relation $T_{LM}T_{ML}=1-r_{LM}^2$, we can rewrite Eq. (10) as

$$\frac{A_{tnsg}^{norm}*A_{dg}^{norm}}{A_{sb}^{norm}*A_{db}^{norm}}=-e^{-4\frac{t_1 2\pi f_0}{Q_L}}\left(1-r_{LM}^2\right). \tag{11}$$

Eqs. (4) and (11) can be solved to give the Q-value of the left layer and the zero-offset plane-wave reflection coefficient of the left interface. In the next section, we use these two relations with ultrasonic laboratory data.

3. Ultrasonic laboratory results

The laboratory data are acquired on a sample consisting of an aluminum (Al) block and a polyvinyl chloride (PVC) block coupled together using an acoustic couplant, see Fig. 2. A second reflective boundary is created by making a groove in the Al block (indicated by the vertical white line in Fig. 2) that is parallel to the PVC/Al interface and 30.5 mm from the interface. The groove is approximately 2 mm wide

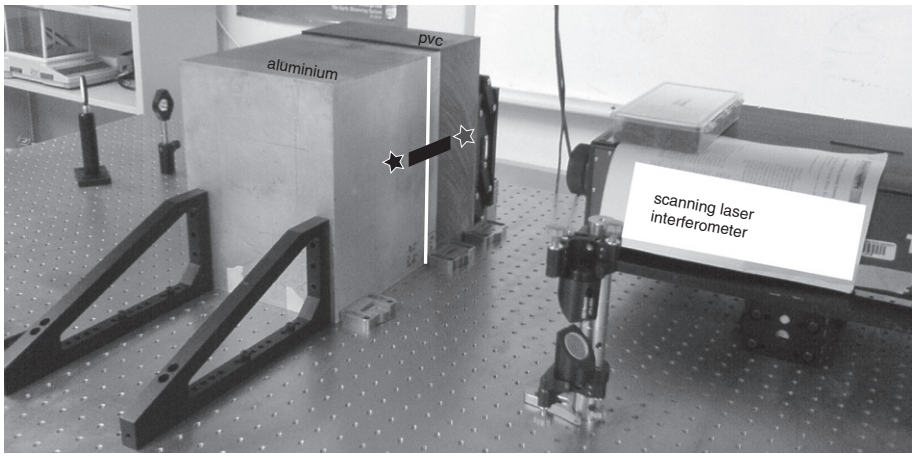

Fig. 2. Laboratory setup used to measure surface waves. The sample consists of aluminum and polyvinyl chloride (PVC) blocks coupled together using an acoustic couplant. The measurements are taken along a line inside the black rectangle using a scanning laser interferometer. A P-wave transducer serves as the seismic source (the black and gray stars). The vertical white line indicates the groove in the aluminum block.

and 10 mm deep. The surface-wave source is a P-wave transducer set at 2 MHz and 400 V and attached to the blocks using acoustic couplant. The source is placed on the Al block 43 mm from the groove (black star in Fig. 2); on the PVC block, the source is placed 45 mm from the PVC/Al interface (gray star in Fig. 2); from now on, we call the two sources Al source and PVC source, respectively. We measure the displacement as a function of time in a direction perpendicular to the measuring surface at 701 points. The measurements are performed using a scanning laser interferometer, based on a constant-wave 250 mW Nd:YAG laser at 532 nm with a flat response between 20 kHz and 20 MHz (see Blum et al., 2010). The measurement line, indicated in Fig. 2 by the black rectangle, starts at 31.6 mm from the PVC/Al interface (13.4 mm from the PVC source), crosses the interface and the groove, and terminates 26.8 mm away from the groove (16.2 mm from the Al source). The spacing between the measurement points along the line is 0.127 mm (0.05 in.) and the time sampling is 50 ns. To increase the strength of the signal received by the laser interferometer, at the points of measurement on the PVC block's surface we glued a thin reflective tape; the signal strength from the Al block was sufficient and thus no reflective tape was needed. Despite the high center frequency of the source transducer, the actually recorded surface-wave energy at the majority of the receiver points from the PVC source is lower than 600 kHz and from the Al source is lower than 1 MHz.

Fig. 3(a,b) shows the measured responses along the line from the PVC and the Al sources, respectively. We can see that the response from the PVC source exhibits arrivals whose frequency content is generally lower than the content of the arrivals from the Al source. This is due to the longer propagation of the waves though the PVC when the source is placed on that block; consequently, there is stronger damping due to the intrinsic losses inside the PVC. The waves experience very little damping when propagating through the Al. The Q-value of Al is about 150,000 Johnston and Toksöz, 1980 and for practical purposes this material can be considered as not causing intrinsic losses. We chose to use Al as a second part of the sample exactly because of this, so that the multiple scattered arrivals do not weaken too quickly to the noise level.

To estimate the Q-value of the PVC and the reflection coefficient of the PVC/Al interface, we use the recorded surface waves. We record the vertical particle displacement, so the surface waves are Rayleigh waves. These are the most energetic arrivals from both sources. In Fig. 3(a) the direct surface wave (labeled with i) from the PVC source is recorded at the left-most receiver (first trace) at around 0.014 ms and at the right-most trace (trace 701) at around 0.067 ms (using the black, i.e. the positive peak); in Fig. 3(b) the direct surface wave from the Al source is recorded at the right-most trace at around 0.0062 ms and at the left-most trace at around 0.059 ms. For the PVC source, the Rayleigh wave reflected from the PVC/Al interface (labeled with ii) is clearly observable and is recorded at the left-most trace at around 0.077 ms. Because the source–receiver line is perpendicular to the interface, the reflected Rayleigh wave will have the same moveout as the direct Rayleigh wave. For the same source, the Rayleigh wave reflected

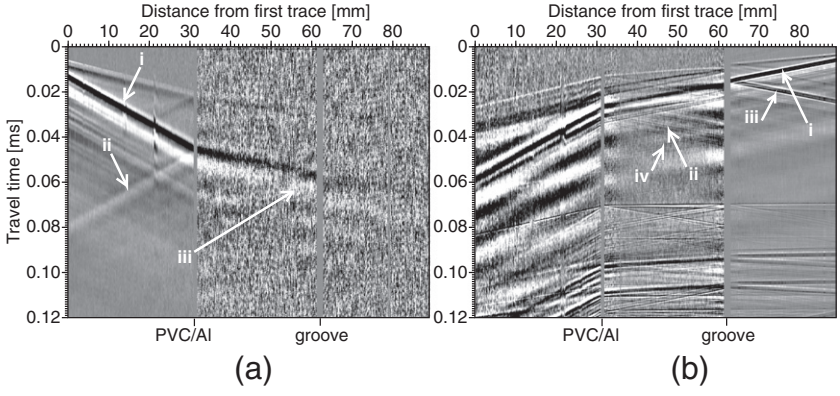

Fig. 3. Recorded responses along the measurement line from the (a) PVC source and (b) Al source. For visualization purposes, each trace in both images has been normalized to its maximum and additionally the images have been clipped. The surface-wave arrivals are labeled as follows: direct — i; reflection from the PVC/Al interface — ii; reflection from the groove — iii; internal reflection between the PVC/Al interface and the groove — iv.

from the groove (labeled with iii) is barely observable. For the Al source, the Rayleigh wave reflected from the PVC/Al interface is clearly observable until it reflects from the groove (labeled with iv), after which it becomes nearly uninterpretable. There are also P-to-surface-wave conversions from the sample's PVC vertical limit due to the PVC source and from the Al vertical limit due to the Al source. These conversions exhibit the same move out as the direct Rayleigh arrival. The arrivals from the limits are weak but, nevertheless, interfere with the reflections from the PVC/Al interface and the groove. There are also surface-wave reflections from the vertical limits. The direct P-waves (the arrivals in Fig. 3(a,b) recorded earlier than the direct Rayleigh waves) and their transmissions, reflections and conversions to surface waves are also observable. The P-wave conversions to Rayleigh waves at the PVC/Al interface and the groove interfere with the direct Rayleigh waves. For the Al source, P-wave reflections from the bottom of the sample are clearly visible (the nearly horizontal arrivals to the right of the PVC/Al interface). These arrive later in time and do not interfere with the Rayleigh waves we want to use for the estimation of Q and the reflection coefficient.

The surface waves caused by the left and right vertical limits of the sample interfere with the reflected Rayleigh waves from the PVC/Al interface and the groove and might result in erroneous estimation of the Q (using both our method and the spectral-ratio method) and the reflection coefficient. We attempt to minimize the influence of the surface-wave reflections from the left vertical boundary. For this, we use the fact that due to their longer propagation, these reflections would be characterized by lower frequencies than the arrivals we want to use. Because of this, we band-pass filter the recordings between 110 kHz and 300 kHz. This filter is chosen such that the Rayleigh waves reflected between the PVC/Al interface and the groove from both sources would still remain in the filtered result. The filtered responses are shown in Fig. 4(a,b). Because we use Rayleigh waves for the estimation of Q and the reflection coefficient, for both sources we mute all arrivals earlier than the direct Rayleigh wave. Even though in the filtered results from both sources the reflection from the groove (the arrival at 0.057 ms and 0.037 ms in Fig. 4(a,b), respectively, and propagating to the left of the groove) is still weak, now it is more easily interpretable on the traces to the left of the groove.

In Fig. 4(a,b), just like in Fig. 3(a,b), the individual traces are normalized with the amplitude of the direct Rayleigh arrival. In our case, this is the maximum amplitude of each trace. As explained in the previous section, this normalization is needed to account for the different intrinsic losses during propagation of the Rayleigh waves from the PVC and the Al sources to the receivers. The normalization also accounts for possible differences in the amplitudes of the sources, which might be the case in our measurements because the source coupling to the PVC and Al is not necessarily the same.

We can see that the band-pass filtering suppresses some of the arrivals caused by the PVC and Al vertical limits of the sample, but does not eliminate all of them. In Fig. 4(a,b) we can still see surface-wave energy caused by the PVC and Al sample limits.

To identify if a ghost reflection is present in the results retrieved from seismic interferometry, and to possibly tie it to the layer between the PVC/Al interface and the groove (from which we expect to have a ghost reflection), we need the Rayleigh-wave reflections from the PVC/Al interface and the groove. These are weak compared to some of the Rayleigh-wave arrivals from the PVC and Al vertical sample limits. In the correlation process of seismic interferometry, correlation with and among the arrivals from the sample's physical limits results in relatively strong spurious events that in the summation process will increase or decrease the amplitudes of the ghost reflections we are after and thus might result in the ghosts having erroneous polarity. To avoid that, we further mute all arrivals that are not expected to contribute to the retrieved ghost reflection for our geometry. The result is shown in Fig. 5(a,b). The remaining arrivals in the figure can be explained using the parallels with the cartoon from Fig. 1. The PVC source acts as the gray source, while the Al source acts as the black source. To the left of the PVC/Al interface, the kept arrivals from the PVC source are the reflection from the PVC/Al interface (labeled ii), arriving at the left-most trace at around 0.078 ms, and the reflection from the groove (labeled iii), arriving at around 0.099 ms. These two arrivals correspond to the thin solid gray and the dashed gray arrivals in Fig. 1, respectively. For the traces in the same region, the kept events coming from the Al source are the direct Rayleigh wave (labeled i), arriving at the left-most trace at around 0.059 ms, and its multiple that has bounced between the PVC/Al interface and the groove (labeled iv), arriving at around 0.080 ms. These two arrivals correspond to the solid black and dashed black arrivals in Fig. 1, respectively. Between the PVC/Al interface and the groove, the kept events due to both sources are the direct Rayleigh waves and their first internal multiples.

To the right of the groove, the kept events are the opposite of the ones kept to the left of the PVC/Al interface: for the Al source we keep the reflection from the groove and the reflection from the PVC/Al interface, which arrive at the right-most trace at around 0.025 ms and 0.046 ms, respectively; for the PVC source we try to keep the direct Rayleigh wave and its first multiple that has bounced between the PVC/Al interface and the groove. These latter two arrivals, though, are already at the noise level and are interpretable only by following the moveout of the corresponding arrivals recorded to the left of the groove.

To retrieve the ghost reflection due to the layer between the PVC/Al interface and the groove, we autocorrelate trace by trace the two panels in Fig. 5. The identification of the ghost reflection can be done using any of the two autocorrelated panels. Because the signal-to-noise ratio of

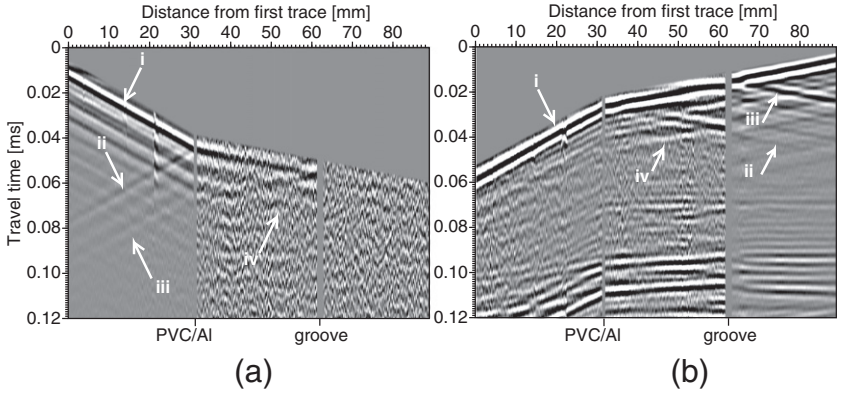

Fig. 4. Recorded responses along the measurement line after band-pass filtering between 110 kHz and 300 kHz from the (a) PVC source and (b) Al source. All arrivals earlier than the direct Rayleigh wave are muted. For visualization purposes, each trace in both images has been normalized to its maximum and then the images have been clipped. The surface-wave arrivals are labeled as in Fig. 2.

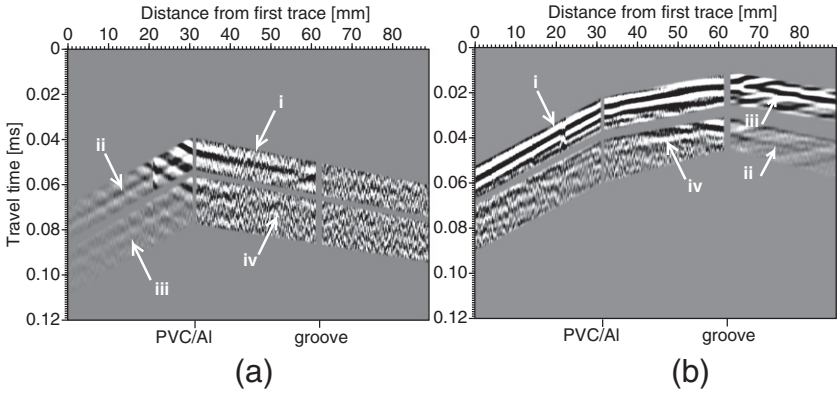

Fig. 5. As in Fig. 3 but after muting all arrivals that are not expected to contribute to the retrieval of the ghost reflection between the PVC/Al interface and the groove.

the reflected surface waves is higher for the Al source, we use this autocorrelated result, see Fig. 6(a). For visualization purposes, each trace is normalized with its maximum. The expected arrival time of the ghost reflection is indicated by the solid rectangle for receivers to the right of the groove and with dashed rectangle for receivers to the left of the groove. We can see that to the right of the groove the ghost reflection predominantly exhibits a white–black–white wavelet, while left of the groove the ghost clearly exhibits a wavelet with the opposite polarity of black–white–black. The change in polarity of the retrieved ghost Rayleigh-wave reflection can be exemplified by stacking the traces in Fig. 6(a) to the left and to the right of the groove. The stacked traces passing through the solid rectangle result in the solid trace in Fig. 6(b), while the stacked traces passing through the dashed rectangle — in the dashed trace in Fig. 6(b). We can observe that around 0.020 ms the polarities of the stacked traces are indeed reversed. The change in the polarity of the retrieved ghost reflection on both sides of the groove confirms that this ghost is produced by the multiple bouncing of the surface waves between the PVC/Al interface and the groove. This means that in a consecutive estimation procedure, the Q-value of the layer to the left of the PVC/Al interface and the reflection coefficient of the PVC/Al interface will be estimated if receivers to the left of the PVC/Al interface are used; if receivers to the right of the groove are used, then the Q-value of the layer to the right of the groove and the reflection coefficient of the groove will be estimated.

In this result, we know around which time we should expect the ghost reflection, as we use data from a controlled laboratory experiment. We know the distance between the interface and the groove, while the Rayleigh-wave velocities in the PVC and in the Al are calculated using the travel-time difference of the direct Rayleigh wave between the receivers (2900 m/s for the Al and 990 m/s for the PVC). For the same reason, we know which arrivals in the panels in Fig. 4 should be muted to obtain the panels in Fig. 5. With field data, where physical limits of a "sample" would not be present, such calculations would not be needed. The recordings at different traces from two sources should be directly autocorrelated. Possible ghost reflections should then be identified and distinguished from physical reflections directly from changes in the polarity of traces from receivers at different sides of possible structural boundaries. Once a ghost reflection is identified, if the surface-wave velocity inside the structure causing the ghost is known, the thickness of that structure can be calculated using the two-way travel time of the ghost reflection.

Now that the ghost reflection has been identified and tied to the layer between the PVC/Al interface and the groove, we proceed to estimate the Q-value of the PVC and the reflection coefficient at the interface. We do this using Eqs. (4) and (11):

$$A_{tnsg}^{norm} = e^{-2\frac{t_1 2\pi f_0}{Q_{PVC}}} r_{PVC/Al}, \tag{12}$$

where A_{tnsg}^{norm} correspond to the normalized reflected Rayleigh wave due to the PVC source, t_1 corresponds to the one-way travel time of the Rayleigh wave from the measurement point to the PVC/Al interface,

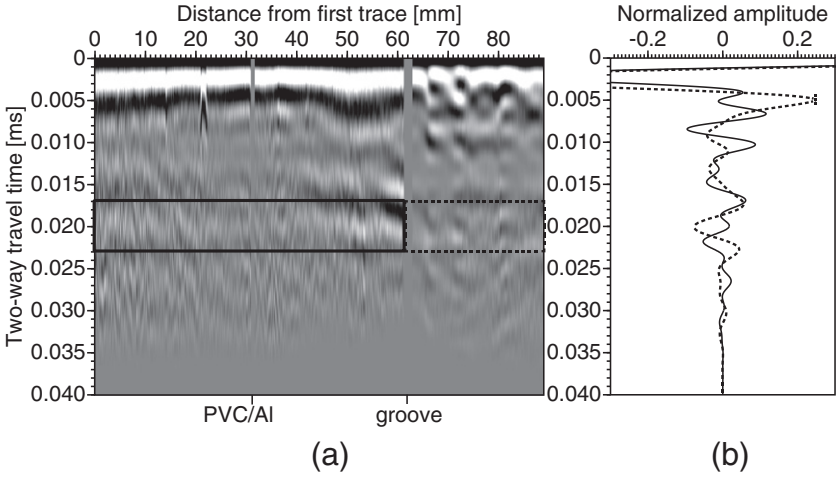

Fig. 6. (a) Result from the applying autocorrelation to the muted source response in Fig. 4(b). The solid and dashed rectangles indicate the expected time of the retrieved ghost Rayleigh-wave reflections caused by the layer between the PVC/Al interface and the groove. For visualization purposes, each trace has been normalized by its maximum. (b) Result from the stacking of the traces in (a) that pass through the solid rectangle (solid) and through the dashed rectangle (dashed).

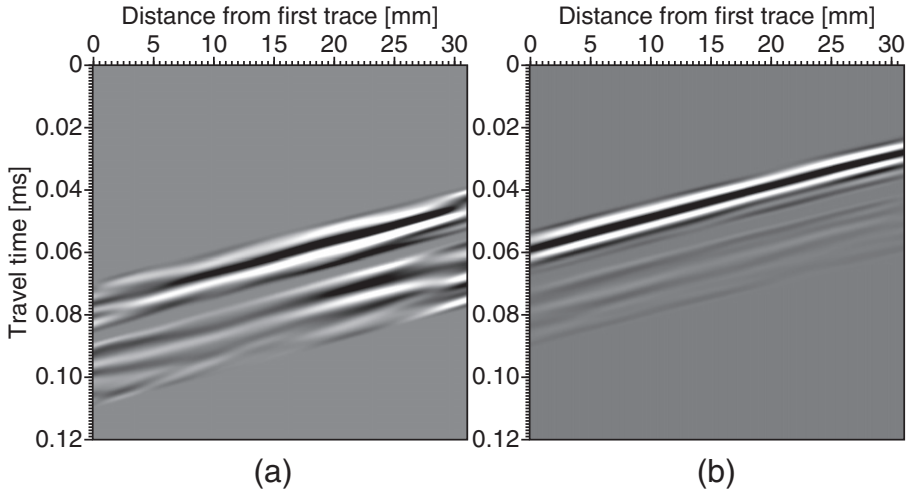

Fig. 7. As in Fig. 4 but after application of a frequency-wavenumber fan filter and only for the traces to the left of the PVC/Al interface.

and we have exchanged L with PVC and LM with PVC/Al;

$$\frac{A^{norm}_{tmsg} * A^{norm}_{dg}}{A^{norm}_{sb} * A^{norm}_{db}} = -e^{-4\frac{t_1 2\pi f_0}{Q_{PVC}}}\left(1-r^2_{PVC/Al}\right), \tag{13}$$

where A^{norm}_{dg} corresponds to the Rayleigh wave reflected from the groove due to the PVC source, while A^{norm}_{sb} and A^{norm}_{db} are the direct Rayleigh wave due to the Al source and its multiple that has bounced between the PVC/Al interface and the groove, respectively.

The values of the amplitudes for the ratio in Eq. (13) can be taken from the autocorrelation results (before summation over the two sources) at the two-way travel time of the identified ghost for any receiver position inside the layer whose Q-value is sought. The accuracy of those values, though, might be affected by interference with artifacts from the correlation of other events, which may be very weak, but whose arrival time coincides with the arrival time of the ghost reflection. Because of this, here we prefer to pick the amplitudes needed for the calculation of the left-hand side in Eq. (13), but also in Eq. (12), directly from the normalized data. This can be done using the panels in Fig. 5. In those panels, though, especially for the panel in Fig. 5(a), we can see that there is interference from arrivals due to the PVC vertical boundary of the sample. Because we need to pick amplitudes only for arrivals recorded to the left of the PVC/Al interface, we apply frequency-wavenumber filtering to the recordings in Fig. 5. We use the fact that for the source on the PVC (Fig. 5(a)), the reflected Rayleigh waves from the PVC/Al interface and from the groove are propagating in a direction opposite to the direction of the Rayleigh waves reflected from the PVC vertical limit of the sample. This means that in the frequency-wavenumber domain these two types of Rayleigh-wave arrivals will be on opposite sides of the zero wavenumber and thus could be easily separated by a fan filter. For the source on the Al, P-waves that convert to Rayleigh waves at the Al vertical limit of the sample will have the same propagation direction (and inclination) as the direct and reflected Rayleigh waves we want to use. Because of this, a frequency-wavenumber fan filter for this source would only eliminate the week P-waves. The surface-wave arrivals we want to use for the estimation might still suffer from week interference from the conversions at the Al vertical limit of the sample. The results of the application of the frequency-wavenumber filtering are shown in Fig. 7(a,b). We show only traces to the left of the PVC/Al interface, because receivers to the left of the interface are need for the estimation of Q_{PVC} and $r_{PVC/Al}$. We see that some of the interfering events, especially those caused by the PVC vertical limit are removed.

The above derivations supposed plane-wave sources. In our case, the sources do not excite plane waves, so we apply a surface-wave geometrical-spreading correction to the picked values. We calculate results for recordings at several receivers, namely at distances from the left-most receiver of 7.37 mm, 9.91 mm, 12.45 mm, 14.99 mm, and 18.80 mm (corresponding to traces 59, 79, 99, 119, and 149). The estimated Q-values and reflection coefficients at the PVC/Al interface for these traces are given in Table 1 (second and third rows). In the right-most columns, we also give the calculated average and the standard deviation σ. It can be seen that the estimated values for the different traces are all close to each other and have little scatter around the average.

As we propose our method as an alternative to the spectral-ratio method and to be used as an independent control, we also estimate the Q-value of the PVC using the spectral-ratio method (e.g. Jannsen et al., 1985; Tonn, 1991). We estimate Q_{PVC} at a measurement point using the reflection from the PVC/Al interface and the direct Rayleigh arrival. We use the exact relation between Q and the slope m of the spectral ratio, which is measured as a function of frequency:

$$Q = \frac{2\pi}{1-e^{-\frac{2m}{2t_1}}}, \tag{14}$$

where t_1 is, just like above, the one-way travel time between the measurement point and the PVC/Al interface. Note that we take for convenience the slope from the negative logarithm of the ratio and so the exponential on the right-hand side is also negative. Fig. 8 shows the individual amplitude spectra of the direct Rayleigh arrivals from the PVC source at the measurement points corresponding to the traces 59, 79, 99, 119, and 149. The values of Q_{PVC}, given in Table 1 (fourth row), are estimated from the slopes as given in Fig. 9. Also here we use arrivals after application of the band-pass filtering between 110 kHz and 300 kHz and the frequency-wavenumber filtering that aim to suppress interfering events.

It can be seen from Table 1 (fourth row) that the average Q_{PVC} estimated with the spectral-ratio method is 13.24, which is about 7%

Table 1
Estimated quality factor Q_{PVC} and reflection coefficients $r_{PVC/Al}$ at the PVC/Al interface. The reflection coefficients in the third row and the Q-values in the second row are estimated using the method we propose, while the Q-values in the fourth row are estimated using the slopes of the spectral ratios (SR) from Fig. 9. The last two columns show the average and the standard deviation (σ) for the values from the separate traces.

Trace number	59	79	99	119	149	Average	σ
Q_{PVC}	12.47	13.18	12.09	12.06	11.92	12.35	0.46
$r_{PVC/Al}$	0.55	0.52	0.53	0.50	0.48	0.51	0.02
Q_{PVC} from SR	14.75	13.05	12.78	13.17	12.45	13.24	0.79

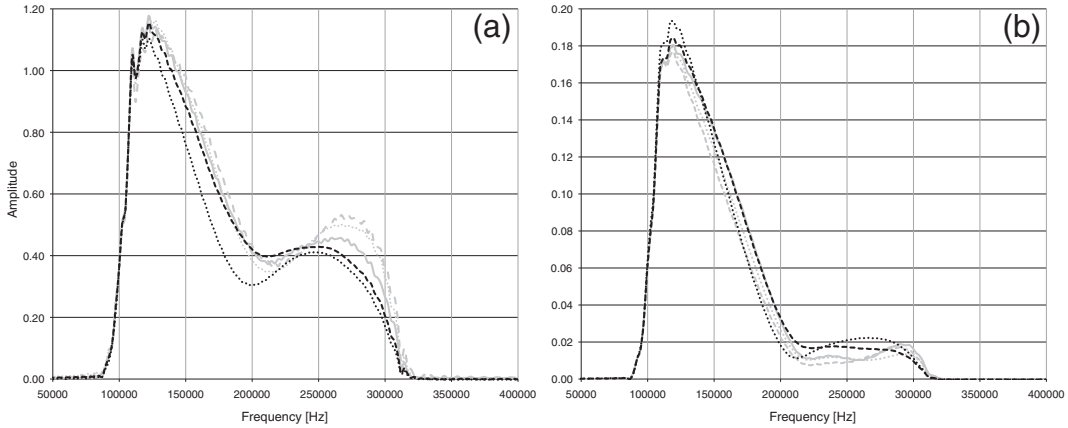

Fig. 8. Amplitude spectrum of the (a) direct Rayleigh waves and (b) their reflections from the PVC/Al interface from the PVC source at traces 59 (dashed gray), 79 (dotted gray), 99 (solid gray), 119 (dashed black), and 149 (dotted black). Note the difference in the amplitude scales in (a) and (b).

higher than the average value obtained using the method we propose as given in the second row in Table 1. Note that the one-σ intervals around the averages from the two methods actually overlap, and that the spectral-ratio results exhibit higher scatter around their average compared to the ghost-reflection results.

In our case, the PVC block is effectively homogeneous and both the method we propose and the spectral-ratio method estimate only damping due to the intrinsic losses, i.e. Q. If the PVC block were also causing scattering losses between the receivers and the PVC/Al interface, both methods would have estimated an effective Q that would represent the intrinsic losses and the scattering losses. The seismic-interferometry theory for a losses medium shows that the exact Green's function will be retrieved when the sources effectively surround the receivers, even in the presence of scattering losses. This signifies that when the medium causes intrinsic losses, the ghost reflection that would be retrieved will be caused only by the intrinsic losses. In our case of approximately 1D laboratory sample, the receivers would be effectively enclosed by the two sources if the sources were indeed emitting plane waves. In such case, application of the Q-estimation procedure as proposed by Draganov et al. (2010), i.e. autocorrelating the complete records at the receivers that included many internal reflections between the PVC/Al interface and the groove, would estimate Q only due to the intrinsic losses even if scattering losses are present between the receivers and the PVC/Al interface. Because here we propose an alternative estimation procedure, that uses only the earliest internal multiple, our estimated Q would also include the possible present scattering losses.

We also calculate the expected reflection coefficient of the PVC/Al interface using the calculated velocities of the direct Rayleigh arrivals in the PVC (990 m/s) and the Al (2900 m/s) and taking the densities of the two materials from the literature — 1360 kg/m^3 and 2700 kg/m^3, respectively. Using these values, we obtain a theoretical value of the reflection coefficient of 0.71. The average of the estimated reflection-coefficient values in Table 1 is 0.51 and is lower than the theoretically expected value. This is an indication that the PVC/Al interface is imperfectly welded. It still needs to be investigated what is the influence of imperfectly welded boundaries on the estimation procedure using Eqs. (4) and (11).

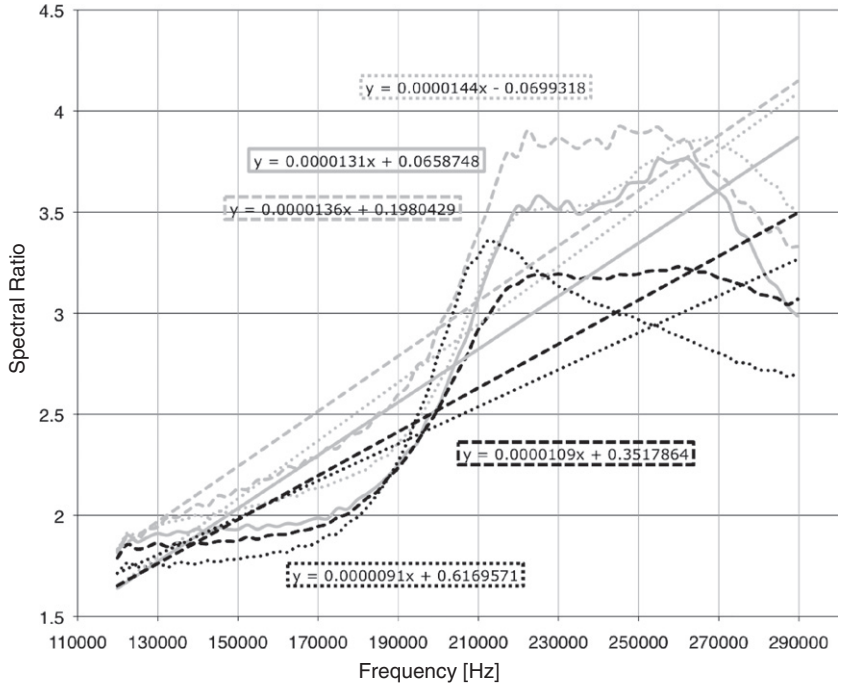

Fig. 9. Spectral ratios (from the reflected and direct arrivals) and their slopes for traces 59 (dashed gray), 79 (dotted gray), 99 (solid gray), 119 (dashed black), and 149 (dotted black).

The above results are obtained for surface-wave arrivals that do not experience dispersion, because the sample was vertically homogeneous. For field applications, layering would be present in the subsurface and will cause dispersive waves to be recorded. The method can easily be adapted to such cases. For this, the recorded arrivals can be filtered between narrow frequency bands and the method is to be applied to each of the bands. In such a way, one can estimate frequency-dependent Q and reflection coefficients.

The comparison of the results using surface waves from our method and the spectral-ratio method validates our method. The method can be applied in the same way to P- and S-wave measurements at the surface from surface sources, for the estimation of Q and reflection coefficient for P- and S-waves, respectively. The method can also be applied to borehole measurements with sources and receivers along the borehole. As we adapted our method from the one proposed by Ruigrok (2012) for body waves, also the latter method is validated with these laboratory results and thus Q- and reflection-coefficient estimation can be applied to surface registrations of earthquakes arriving nearly vertically or to measurements along a horizontal or deviated well from surface sources.

4. Conclusions

We propose a method that uses surface waves reflected from subvertical interfaces to estimate the quality factor of the medium and the reflection coefficient at the subvertical interface. The method uses non-physical (ghost) surface-wave reflections obtained by seismic interferometry by correlation applied to recordings from two transient sources. The ghost reflections are retrieved using internal reflections of the surface waves between two subvertical boundaries. Using ultrasonic laboratory data, we show how the method can be applied in practice. The data was recorded on a sample consisting of a PVC block and an aluminum (Al) block coupled together. The Al block contained a groove, which was parallel to the PVC/Al interface. We use the internal multiple between the PVC/Al interface and the groove to retrieve a Rayleigh-wave ghost reflection. We demonstrate how this ghost reflection can be identified as such due to its change of polarity when retrieved at receivers on opposite sides of the groove. Using the amplitudes of the events that contribute to the retrieval of the identified ghost reflection, we estimate the quality factor of the PVC to be 12.35 and the reflection coefficient at the PVC/Al interface to be 0.51. The reflection coefficient is smaller than the calculated theoretical value of 0.71, indicating an imperfectly welded interface. We also estimate the quality factor of the PVC to be 13.24 using the spectral-ratio method. The two estimated values of the quality factor are very close to each other, thus we confirm that our new approach is a viable alternative.

Acknowledgements

The research of D.D. is supported by CATO2 and by the Division for Earth and Life Sciences (ALW) with financial aid from the Netherlands Organization for Scientific Research (NWO) with VIDI grant 864.11.009. We thank Thomas Blum for his help during the acquisition of the data and guidance with the laser system.

References

Aki, K., Richards, J.P., 2002. Quantitative Seismology. 2nd ed. University Science Books.
Blum, T.E., van Wijk, K., Pouet, B., Wartelle, A., 2010. Multicomponent wavefield characterization with a novel scanning laser interferometer. Rev. Sci. Instrum. 81, 073101.
Campillo, M., Paul, A., 2003. Long-range correlations in the diffuse seismic coda. Science 299, 547–549.
Draganov, D., Ghose, R., Ruigrok, E., Thorbecke, J., Wapenaar, K., 2010. Seismic interferometry, intrinsic losses and Q-estimation. Geophys. Prosp. 58, 361–373.
Draganov, D., Heller, K., Ghose, R., 2012. Monitoring CO_2 storage using ghost reflections retrieved from seismic interferometry. Intern. J. Greenh. Gas Control 11S, S35–S46.
Draganov, D., Ghose, R., Heller, K., Ruigrok, E., 2013. Monitoring of changes in velocity and Q in reservoirs using non-physical arrivals in seismic interferometry. Geophys. J. Int. 192.
Ghose, R., Carvalho, J., Loureiro, A., 2013. Signature of fault zone deformation in near-surface soil visible in shear wave seismic reflections. Geophys. Res. Lett. 40, 1074–1078.
Jannsen, D., Voss, J., Theilen, F., 1985. Comparison of methods to determine q in shallow marine sediments from vertical reflection seismograms. Geophys. Prosp. 33, 479–497.
Johnston, D.H., Toksöz, M.N., 1980. Ultrasonic p and s wave attenuation in dry and saturated rocks under pressure. J. Geophys. Res. 85 (B2 (II)), 925–936.
Kimman, W.P., Trampert, J., 2010. Approximations in seismic interferometry and their effects on surface waves. Geophys. J. Int. 182, 461–476.
King, S., Curtis, A., 2012. Suppressing nonphysical reflections in Green's function estimates using source–receiver interferometry. Geophysics 77, Q15–Q25.
King, S., Curtis, A., Poole, T.L., 2011. Interferometric velocity analysis using physical and nonphysical energy. Geophysics 76, SA35–SA49.
Klimentos, T., 1995. Attenuation of p- and s-waves as a method of distinguishing gas and condensate from oil and water. Geophysics 60, 447–458.
Portsmouth, I.R., Worthington, M.H., Neep, J.P., 1993. A field study in seismic attenuation in layered sedimentary rocks — II. Crosshole data. Geophys. J. Int. 113, 135–143.
Ruigrok, E., 2012. Body-Wave Seismic Interferometry Applied to Earthquake- and Storm-Induced Wavefields. Ph.D. thesis. Delft University of Technology.
Schuster, G.T., 2001. Theory of daylight/interferometric imaging: tutorial. 63rd Conference and Exhibition Extended Abstracts. EAGE, p. A-32.
Schuster, G.T., Yu, J., Rickett, J., 2004. Interferometric/daylight seismic imaging. Geophys. J. Int. 157, 838–852.
Snieder, R., 2004. Extracting the Green's function from the correlation of coda waves: a derivation based on stationary phase. Phys. Rev. E. 69, 046610.
Snieder, R., Wapenaar, K., Larner, K., 2006. Spurious multiples in seismic interferometry of primaries. Geophysics 71, SI111–SI124.
Solomon, S., 1972. Seismic-wave attenuation and partial melting in the upper mantle of North America. J. Geophys. Res. 77, 1483–1502.
Tonn, R., 1991. The determination of the seismic quality factor Q from VSP data: a comparison of different computational methods. Geophys. Prosp. 39, 1–27.
Wapenaar, K., 2004. Retrieving the elastodynamic Green's function of an arbitrary inhomogeneous medium by cross-correlation. Phys. Rev. Lett. 93, 254301.
Wapenaar, K., Thorbecke, J., Draganov, D., Fokkema, J., 2002. Theory of acoustic daylight imaging revisited. 72nd Annual International Meeting Expanded Abstracts. SEG, p. ST 1.5.
Zhubayev, A., Ghose, R., 2012 aa. Contrasting behavior between dispersive seismic velocity and attenuation: advantages in subsoil characterization. J. Acoust. Soc. Am. 131, EL170–EL176.
Zhubayev, A., Ghose, R., 2012 bb. Physics of shear-wave intrinsic dispersion and estimation of in-situ soil properties: a synthetic VSP appraisal. Near Surf. Geophys. 10, 613–629.